The Active Role of the Water Solvent in the Regioselective C═O Hydrogenation of Unsaturated Aldehydes by [RuH_2(*m*tppms)$_x$] in Basic Media

Andrea Rossin,[†] Gábor Kovács,[†,‡,§] Gregori Ujaque,[†] Agustí Lledós,*[,†] and Ferenc Joó*[,‡,§]

Departament de Química, Universitat Autònoma de Barcelona, 08193 Bellaterra (Barcelona), Spain, Institute of Physical Chemistry, University of Debrecen, Debrecen 10, P.O. Box 7, H-4010 Hungary, and Research Group of Homogeneous Catalysis, Hungarian Academy of Sciences, Debrecen 10, P.O. Box 7, H-4010 Hungary

Received April 21, 2006

The regioselective hydrogenation of cinnamaldehyde in basic aqueous media catalyzed by [RuH_2(*m*tppms)$_x$] [x = 3,4; *m*tppms = *meta*-sulfonatophenyl-diphenylphosphine] is analyzed by means of theoretical calculations. The water solvent is modeled by the inclusion of a $(H_2O)_3$ cluster in addition to a continuum model. Two Ru complexes are evaluated as active species for the reduction process: the major identified species [RuH_2P_4] and the related phosphine dissociated complex [RuH_2P_3]. Several reaction mechanisms are computationally evaluated, and their analysis suggests that the reaction takes place in several steps. The first hydrogenation process takes place by means of a hydrogen transfer from the metal catalyst, whereas the second hydrogenation process is performed by a water solvent molecule. This mechanism can account for the selectivity of the C═O versus C═C double bond reduction experimentally observed under basic reaction conditions and can be directly related to the mechanism found in acidic media, where the opposite regioselectivity (C═C vs C═O) is observed.

Introduction

A very important industrial reaction for the production of drugs, flavors, and materials is the hydrogenation of the carbonyl moiety of aldehydes and ketones, to obtain the corresponding alcohol. Classical homogeneous hydrogenation catalysts are often based on Rh or Ru, since many complexes of these metals readily undergo insertion reactions into their M−H bonds.[1] Nowadays, among the most active species that can achieve high activity and selectivity for this conversion are ruthenium-based diamino-diphosphine complexes, containing hydride and dihydrogen ligands, developed by Noyori[2] and Morris,[3] though other very active species were also developed.[4−7] Recent works that appeared in the literature concern the analysis of the reaction mechanism and the nature of the intermediates, by both experimental[8] and theoretical[3d,9] means. In addition, it is possible to observe a parallel improvement of the ancillary chelating ligands for these organometallic reactions[3c] or the attempt to find different (and less expensive) transition metals to catalyze the same reaction.[10] Another important (and exploited) field is that of asymmetric hydrogenations using chiral phosphines or amines as ligands coordinated to the metal center.[11]

In all the aforementioned examples, the solvent used is nonaqueous, being mainly either 2-propanol or acetonitrile. To develop a "greener" and more environmentally friendly chemistry, it would be much better to perform the same reactions in a green solvent. Water is definitely the best candidate to play the role. After the first attempts to use water as the main solvent for industrial-scale conversions (which took place in the 1970s for a hydroformylation process[12]), a growing interest in "greener" chemistry has brought a considerable expansion of the research in the field, especially for the last 15 years.[13] Today, examples of water-soluble catalysts and related two-phase catalytic reactions are numerous and well-known.[13−16] When possible,

* To whom correspondence should be addressed. E-mail: agusti@klingon.uab.es (A.L.); fjoo@delfin.unideb.hu (F.J.).
[†] Universitat Autònoma de Barcelona.
[‡] University of Debrecen.
[§] Hungarian Academy of Sciences.

(1) Chaloner, P. A., Esteruelas, M. A., Joó, F., Oro, L. A., Eds. *Homogeneous Hydrogenation*; Kluwer: Dordrecht, 1996.
(2) (a) Sandoval, C. A.; Okhuma, T.; Muñiz, K.; Noyori, R. *J. Am. Chem. Soc.* **2003**, *125*, 13490. (b) Noyori, R.; Ohkuma, T. *Angew. Chem., Int. Ed.* **2001**, *40*, 40.
(3) (a) Abbel, R.; Abdur-Rashid, K.; Faatz, M.; Hazdovic, A.; Lough, A. J.; Morris, R. H. *J. Am. Chem. Soc.* **2005**, *127*, 1870. (b) Clapham, S. E.; Hazdovic, A.; Morris, R. H. *Coord. Chem. Rev.* **2004**, *248*, 2201. (c) Li, T.; Churlaud, R.; Lough, A. J.; Abdur-Rashid, K.; Morris, R. H. *Organometallics* **2004**, *23*, 6239. (d) Abdur-Rashid, K.; Clapham, S. E.; Hazdovic, A.; Harvey, J. N.; Lough, A. J.; Morris, R. H. *J. Am. Chem. Soc.* **2002**, *124*, 15104. (e) Abdur-Rashid, K.; Lough, A. J.; Morris, R. H. *Organometallics* **2001**, *20*, 1047.
(4) (a) Wu, X.; Vinci, D.; Ikariya, T.; Xiao, J. *Chem. Commun.* **2005**, 4447. (b) Ito, M.; Hirakawa, M.; Murata, K.; Ikariya, T. *Organometallics* **2001**, *20*, 379.
(5) (a) Shvo, Y.; Goldberg, I.; Czierkie, D.; Reshef, D.; Stein, Z. *Organometallics* **1997**, *16*, 133. (b) Menashe, N.; Salant, E.; Shvo, Y. *J. Organomet. Chem.* **1996**, *514*, 97.
(6) (a) Larson, A. L. E.; Persson, B. A.; Bäckvall, J.-E. *Angew. Chem., Int. Ed. Engl.* **1997**, *36*, 1211−1212. (b) Persson, B. A.; Larsson, A. L. E.; Ray, M. L.; Bäckvall, J.-E. *J. Am. Chem. Soc.* **1999**, *121*, 1645−1650. (c) Samec, J. S. M.; Él, A. H.; Bäckvall, J.-E. *Chem. Eur. J.* **2005**, *11*, 2327−2334.
(7) (a) Casey, C. P.; Singer, S. W.; Powell, D. R.; Hayashi, R. K.; Kavana, M. *J. Am. Chem. Soc.* **2001**, *123*, 1090. (b) Casey, C. P.; Johnson, J. B.; Singer, S. W.; Cui, Q. *J. Am. Chem. Soc.* **2005**, *127*, 3100. (c) Casey, C. P.; Bikzhanova, G. A.; Cui, Q.; Guzei, I. A. *J. Am. Chem. Soc.* **2005**, *127*, 1883.
(8) Hamilton, R. J.; Leong, C. G.; Bigam, G.; Miskolzie, M.; Bergens, S. H. *J. Am. Chem. Soc.* **2005**, *127*, 4152.
(9) (a) Brandt, P.; Roth, P.; Andersson, P. G. *J. Org. Chem.* **2004**, *69*, 4885. (b) Nordin, S. J. M.; Roth, P.; Tarnai, T.; Alonso, D. A.; Brandt, P.; Andersson, P. G. *Chem. Eur. J.* **2001**, *7*, 1431. (c) Alonso, D. A.; Brandt, P.; Nordin, S. J. M.; Andersson, P. G. *J. Am. Chem. Soc.* **1999**, *121*, 9580.
(10) Bullock, M. R. *Chem. Eur. J.* **2004**, *10*, 2366.
(11) (a) Xu, X.; Vinci, D.; Ikariya, T.; Xiao, J. *Chem. Commun.* **2005**, 4447. (b) Carmona, D.; Lamata, M. P.; Oro, L. A. *Eur. J. Inorg. Chem.* **2002**, 2239.

10.1021/om060353s CCC: $33.50
Publication on Web 09/02/2006

Scheme 1. Hydrogenation of Unsaturated Aldehydes in Water

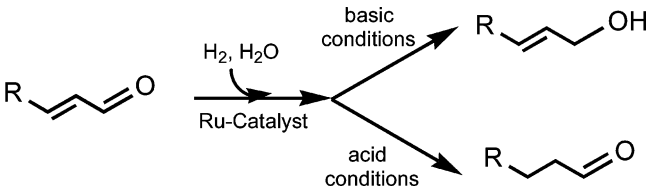

the organic layer is eliminated, to perform the whole transformation in water only. In addition, the biphasic medium allows almost complete recovery of the catalyst itself, thus reducing the amount of toxic (heavy metal-containing) waste.

One of the best examples in this context is offered by the ruthenium(II) system used by Joó et al.,[17] since it performs selective C═C/C═O hydrogenation of α,β-unsatured aldehydes in a biphasic water/chlorobenzene medium (Scheme 1). The active species are water-soluble *m*tppms complexes (*m*tppms = *meta*-sulfonatophenyl-diphenylphosphine). Unfortunately, on the basis of the experimental data, nothing was known about the nature of the various intermediates that form the catalytic cycle; the only experimental information available from NMR data is the nature of the starting active species in both acidic and basic solutions. In fact, it has been proved that the selectivity is related to the presence of *different hydride complexes at different pH values of the water layer*. In other words, the selectivity is pH-related. Similar regioselective hydrogenations of α,β-unsaturated aldehydes were reported by Hernandez and Kalck[13l] and Grosselin et al.[13m]

Our objective was also to apply theoretical methods to cast light on the nature of the catalytic intermediates and transition states, to provide a plausible reaction mechanism. Second, we tried to justify the observed C═C versus C═O reduction selectivity at different pH values. In particular, in this work the results related to the hydrogenation in *basic medium* are presented, where the major ruthenium(II) species that was observed experimentally is *cis*-[RuH_2(*m*tppms)$_4$]. The results related to the hydrogenation in acidic medium are the subject of a separate work.[18] Joubert et al.[19] recently published a study concerning the selectivity for C═O reduction (vs C═C reduction) catalyzed by phosphine complexes of ruthenium in aqueous-biphasic reaction medium, and a comparison of our results and their conclusions is also given.

Computational Details

All DFT calculations used the program package Gaussian03[20] and the B3LYP[21] combination of functionals. The LANL2DZ[22] pseudopotential was employed for the Ru center, and the standard 6-31G(d) basis set was used for the carbon, oxygen, and phosphorus atoms. The 6-31G basis was used on all hydrogens. For all the transition states analytical frequencies were calculated, to check that only one imaginary value is obtained in each case. Normal coordinate analyses were also performed on these saddle points by intrinsic reaction coordinate (IRC) calculations[23] in both directions to the corresponding minima. When the IRC calculations failed to reach the minima, geometry optimizations from the initial phase of the IRC path were performed.

The QM/MM analysis performed on some structures is based on the ONIOM method implemented in Gaussian, with the UFF force field[24] to describe the MM part. The MM treatment was limited to the phenyl rings of the triphenylphosphine ligands of *cis*-[$RuH_2(PPh_3)_4$]. For energy comparisons, single-point calculations at the B3LYP level were carried out on the optimized structures.

As far as the solvent is concerned, its effects were included both by the conductor-like polarizable continuum model (C-PCM UAKS topological model[25]) and by incorporating discrete water molecules in key positions in the optimizations. Solvent calculations with the continuum model were performed at the gas-phase optimized geometries. The discrete model used to represent the aqueous medium consists of a cluster of three neutral molecules $(H_2O)_3$, interbound by hydrogen bonds. A single water molecule does not provide a realistic description of the medium, since proton exchange processes that take place during the catalytic process imply a separation of charges with formation of highly reactive ions. These species (H_3O^+/OH^-) are "stabilized by complexation" through hydrogen bonding to other water molecules.[26] From earlier systematic investigations by Kovács et al.[27] it is shown that a cluster made of three water molecules represents a good compromise

(12) (a) Cornils, B., Herrmann, W. A., Eds. *Applied Homogeneous Catalysis with Organometallic Compounds*; VCH: Weinheim, 1996; Chapter 2.1.1, pp 31−103. (b) Joó, F. *Aqueous Organometallic Catalysis*; Kluwer: Dordrecht, 2001. (c) Van Leeuwen, P. W. N. M., Claver, C., Eds. *Rhodium Catalyzed Hydroformylation*; Kluwer: Dordrecht, 2000.

(13) For general reviews see, for example: (a) Phillips, A. D.; Gonsalvi, L.; Romerosa, A.; Vizza, F.; Peruzzini, M. *Coord. Chem. Rev.* **2004**, *248*, 955. (b) Pinault, N.; Bruce, D. W. *Coord. Chem. Rev.* **2003**, *241*, 1. (c) Gladysz, J. A. *Chem. Rev.* **2002**, *10*, 102. (d) Sinou, D. *Adv. Synth. Catal.* **2002**, *344*, 221. For specific reactions and related catalysts see, for example: (e) Li, X.; Wu, X.; Chen, W.; Hancock, F. E.; King, F.; Xiao, J. *Org. Lett.* **2004**, *6*, 3321. (f) Akbayeva, D. N.; Gonsalvi, L.; Oberhauser, W.; Peruzzini, M.; Vizza, F.; Brüggeller, P.; Romerosa, A.; Sava, G.; Bergamo, A. *Chem. Commun.* **2003**, 264. (g) Saoud, M.; Romerosa, A.; Carpio Mañas, S.; Gonsalvi, L.; Peruzzini, M. *Eur. J. Inorg. Chem.* **2003**, 1614. (h) Joó, F.; Kovács, J.; Bényei, A. Cs.; Nádasdi, L.; Laurenczy, G. *Chem. Eur. J.* **2001**, *7*, 1, (i) Joó, F.; Laurenczy, G.; Karády, P.; Elek, J.; Nádasdi, L.; Roulet, R. *Appl. Organomet. Chem.* **2000**, *14*, 857. (j) Joó, F.; Laurenczy, G.; Nádasdi, L.; Elek, J. *Chem. Commun.* **1999**, 971. (k) Sánchez-Delgado, R. A.; Medina, M.; López-Linares, F.; Fuentes, A. *J. Mol. Catal. A* **1997**, *116*, 167. (l) Hernandez, M.; Kalck, P. *J. Mol. Catal. A: Chem.* **1997**, *116*, 131. (m) Grosselin, J. M.; Mercier, C.; Allmang, G.; Grass, F. *Organometallics* **1991**, *10*, 2126.

(14) Wu, X. F.; Li, X. G.; King, F.; Xiao, J. L. *Angew. Chem., Int. Ed.* **2005**, *42*, 3407.

(15) Ma, Y. P.; Liu, H.; Chen, L.; Cui, X.; Zhu, J.; Deng, J. E. *Org. Lett.* **2003**, *5*, 2103.

(16) Cadierno, V.; Garcia-Garrido, S. E.; Gimeno, J. *Chem. Commun.* **2004**, 232.

(17) Joó, F.; Kovács, J.; Bényei, A. Cs.; Kathó, Á. *Catal. Today* **1998**, *42*, 441. Joó, F.; Kovács, J.; Bényei, A. Cs.; Kathó, Á. *Angew. Chem., Int. Ed.* **1998**, *37*, 969.

(18) Kovács, G.; Ujaque, G.; Lledós, A.; Joó, F. *Organometallics* **2006**, *25*, 862.

(19) Joubert, J.; Delbecq, F. *Organometallics* **2006**, *25*, 854.

(20) Frisch, M. J.; Trucks, G. W.; Schlegel, H. B.; Scuseria, G. E.; Robb, M. A.; Cheeseman, J. R.; Montgomery, J. A.; Vreven, T., Jr.; Kudin, K. N.; Burant, J. C.; Millam, J. M.; Iyengar, S. S.; Tomasi, J.; Barone, V.; Mennucci, B.; Cossi, M.; Scalmani, G.; Rega, N.; Petersson, G. A.; Nakatsuji, H.; Hada, M.; Ehara, M.; Toyota, K.; Fukuda, R.; Hasegawa, J.; Ishida, M.; Nakajima, T.; Honda, Y.; Kitao, O.; Nakai, H.; Klene, M.; Li, X.; Knox, J. E.; Hratchian, H. P.; Cross, J. B.; Adamo, C.; Jaramillo, J.; Gomperts, R.; Stratmann, R. E.; Yazyev, O.; Austin, A. J.; Cammi, R.; Pomelli, C.; Ochterski, J. W.; Ayala, P. Y.; Morokuma, K.; Voth, G. A.; Salvador, P.; Dannenberg, J. J.; Zakrzewski, V. G.; Dapprich, S.; Daniels, A. D.; Strain, M. C.; Farkas, O.; Malick, D. K.; Rabuck, A. D.; Raghavachari, K.; Foresman, J. B.; Ortiz, J. V.; Cui, Q.; Baboul, A. G.; Clifford, S.; Cioslowski, J.; Stefanov, B. B.; Liu, G.; Liashenko, A.; Piskorz, P.; Komaromi, I.; Martin, R. L.; Fox, D. J.; Keith, T.; Al-Laham, M. A.; Peng, C. Y.; Nanayakkara, A.; Challacombe, M.; Gill, P. M. W.; Johnson, B.; Chen, W.; Wong, M. W.; Gonzalez, C.; Pople, J. A. *Gaussian 03*, Revision C.02; Gaussian Inc.: Wallingford, CT, 2004.

(21) (a) Becke, A. D. *J. Chem. Phys.* **1993**, *98*, 5648. (b) Stephens, P. J.; Devlin, J. F.; Chabalowski, C. F.; Frisch, M. J. *J. Phys. Chem.* **1994**, *98*, 11623.

(22) Hay, P. J.; Wadt, W. R. *J. Chem. Phys.* **1985**, *82*, 270.

(23) Fukui, K. *Acc. Chem. Res.* **1981**, *14*, 363.

(24) Rappé, A. K.; Casewit, C. J.; Colwell, K. S.; Goddard, W. A., III; Skiff, W. M. *J. Am. Chem. Soc.* **1992**, *114*, 10024.

(25) Cossi, M.; Rega, N.; Scalmani, G.; Barone, V. *J. Comput. Chem.* **2003**, *24*, 669.

(26) Siegbahn, P. E. M. *J. Comput. Chem.* **1996**, *17*, 1099.

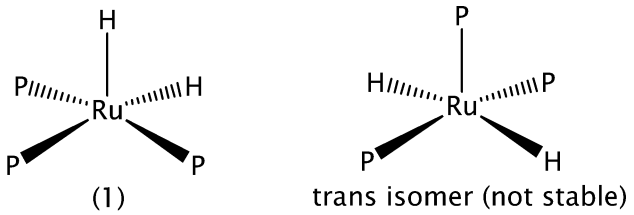

Figure 1. Different isomers of $[RuH_2(PH_3)_3]$.

between a realistic description and system size (and related proportional computational time). All the energy profiles presented in the article include solvent corrections with the continuum model. These calculations were also applied when explicit water molecules were considered (discrete-continuum solvent representation).

Discussion of Results

When the precursor compound $[\{RuCl_2(m\text{tppms})_2\}_2]$ is dissolved in water in the presence of H_2 and an excess of *m*tppms, it undergoes a series of complex equilibria, where proton production is observed.[28] The potentiometric and NMR (^1H and ^{31}P) data revealed the formation of various hydrides, among which the most abundant species were found to be $[RuHCl(m\text{tppms})_3]$ and *cis*-$[RuH_2(m\text{tppms})_4]$ under acidic and basic pH conditions, respectively. The latter complex has a "saturated" octahedral coordination on ruthenium. This complex was found to be active toward selective hydrogenation of the carbonyl group of α,β-unsaturated aldehydes, and the final product is an allylic alcohol.

In the model catalytic complex $[RuH_2(PH_3)_4]$ the "real" water-soluble phosphines were replaced by PH_3, while acrolein was used as a model for cinnamaldehyde.

Two paths for reduction of the carbonyl moiety of acrolein were considered:

(1) "P_3" mechanism: the active species is $[RuH_2(PH_3)_3]$, and this mechanism obviously involves the dissociation of a phosphine ligand. In this case, previous coordination of the carbonyl to the metal is conceivable, since ruthenium has a coordination vacancy, similar to $[RuHCl(PH_3)_3]$, which is the model of the active species in the acidic solution. This kind of mechanism was taken into account due to the fact that previous calculations on the hydrogenation of CO_2 in basic aqueous solutions showed that the catalytically active metal complex was indeed that with "RuH_2P_3" stoichiometry.[27b]

(2) "P_4" mechanism: the active species is $[RuH_2(PH_3)_4]$.

Consequently, the discussion of results will be split into two different subsections. First we consider the "P_3" mechanism, whereas the next subsection is devoted to the "P_4" mechanism.

1. Catalysis with $[RuH_2(PH_3)_3]$ ("P_3" mechanism). 1.1. First Hydrogenation Step: Hydrogen Comes from the Catalyst. The initial active species $[RuH_2(PH_3)_3]$ (**1**, Figure 1) has a coordination vacancy on the metal center, and it could coordinate the C═O group. Initially, the study of catalyst isomerism was carried out, and the results showed that only the *cis* isomer exists in a stable form. The *trans* isomer *converts into the cis one* during the optimization process (Berry pseudorotation) and could not be located as a minimum on the potential energy surface.

For the model complex geometry optimizations of both the "D_{3h}-like" (trigonal bipyramidal) and "C_{4v}-like" (square pyramidal) shapes taken into account for coordination number 5 led to a final square pyramidal structure for this complex. The introduction of the bulkier triphenylphosphine ligands in the calculation to represent the real complex slightly changes the final ligand disposition around the metal center. It gives a distorted square pyramid, as it appears in the ONIOM-optimized structure of **1-PPh$_3$** (see Figure 2 and Supporting Information).

The coordination vacancy is always *trans* to a hydride ligand because of the strong *trans effect* of the hydride substituents. This is confirmed by the calculated values for the phosphine dissociation energy (gas phase) for *cis*-$[RuH_2(PPh_3)_4]$. There are two types of phosphines in this complex, and the dissociation energies are 1.7 and 9.6 kcal/mol for the phosphine in *trans* and *cis* position to a hydride, respectively. This result underlines that phosphine dissociation is more favorable at the *trans*-H position and shows that the pentacoordinated complex is very close in energy to the hexacoordinated one.

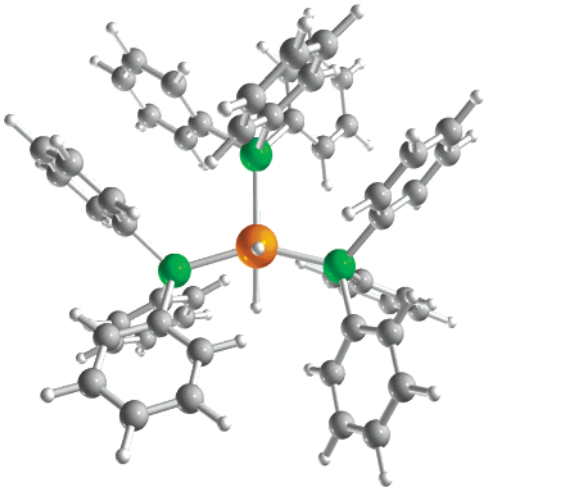

Figure 2. Optimized structure of *cis*-$[RuH_2(PPh_3)_3]$ (view along the pyramidal axis).

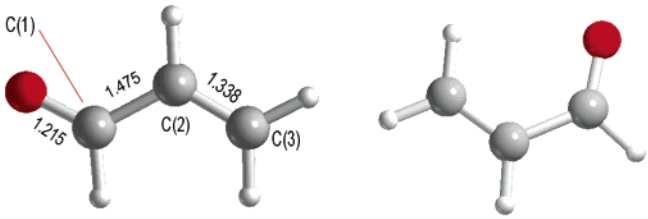

Figure 3. *Transoid* and *cisoid* acrolein [selected optimized bond lengths (Å) are reported]. No substantial differences in the C═O/C═C/C—C bond lengths between the two isomers were found.

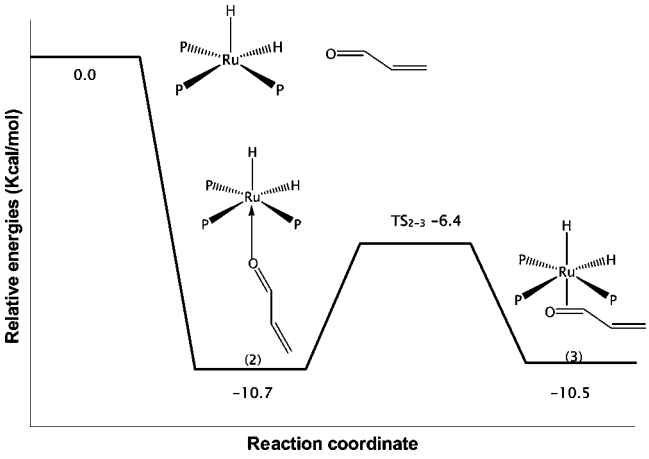

Figure 4. Energy profile for aldehyde coordination through the C═O bond and slippage on **1**.

(27) (a) Kovács, G.; Schubert, G.; Joó, F.; Pápai, I. *Organometallics* **2005**, *24*, 3059. (b) Kovács, G.; Schubert, G.; Joó, F.; Pápai, I. *Catal. Today* **2006**, *115*, 53.

(28) Joó, F. *Acc. Chem. Res.* **2002**, *35*, 738.

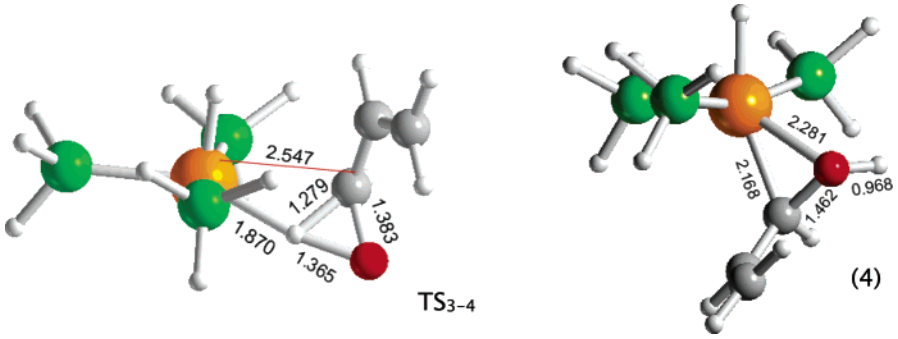

Figure 5. $\mathbf{TS_{3-4}}$ and related complex **4** [selected optimized bond lengths (Å) are reported].

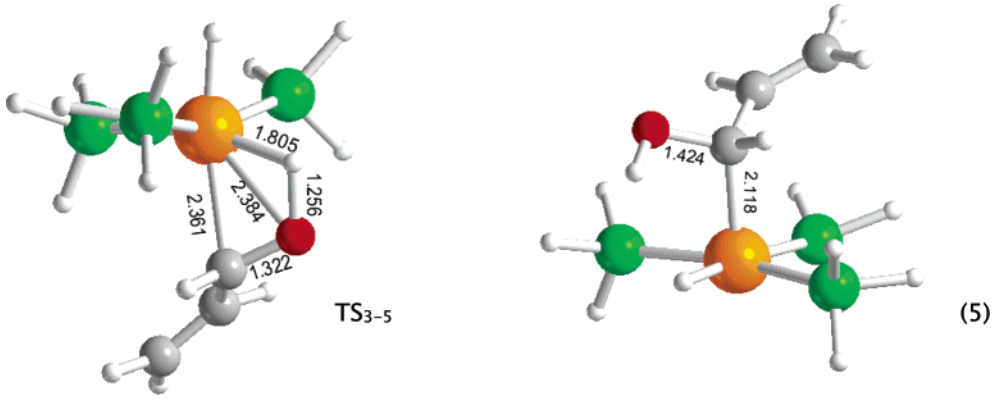

Figure 6. $\mathbf{TS_{3-5}}$ and related complex **5** [selected optimized bond lengths (Å) are reported].

Regarding the organic substrate, different *cisoid* and *transoid* forms of acrolein were also optimized; rotation around the C(1)−C(2) bond leads to several conformational isomers (rotamers, Figure 3). The *transoid* form is more stable by 2.0 kcal/mol; hence it was the isomer of choice for all calculations.

After the phosphine dissociation leading to the catalytically active "RuH_2P_3" species, C═O coordination of acrolein to the metal center was first examined. The structure of [$RuH_2(PH_3)_3$-(acrolein)] was optimized, considering both the η^1-κ,O (**2**) and the η^2-(κ,C-κ,O) (**3**) coordination modes. Even if the η^1 isomer is slightly more stable by 0.2 kcal/mol, the change $\eta^1 \rightarrow \eta^2$ is observed when the O-bound intermediate is formed (vide infra). Figure 4 shows the energy profile for the aldehyde slippage.

For the first hydrogenation step three possibilities were considered: (i) "C(1)-bound" intermediate, where the hydrogen atom binds to the oxygen of the carbonyl group, and a direct Ru−C(1) bond is formed; (ii) "O-bound" intermediate, where the H atom binds to C(1), and a Ru−O bond is formed [the opposite of case (i)]; (iii) "C(3)-bound" intermediate, with initial Michael addition of H^- to the C(3) atom, eventually forming a direct Ru−C(3) bond (vide infra). For the aldehyde atom numbering refer to Figure 3.

(i) In the C(1) case, both the "D_{3h}-like" and the "C_{4v}-like" geometries built at the beginning for complex [$RuH(PH_3)_3$(η^1-κ,C(1)−OH−CH−CH═CH_2)] led to the same final product **4**, with the oxygen atom filling the ruthenium coordination vacancy with a dative O→Ru bond (Figure 5).

The C−O bond is clearly single (cf. the value obtained in *transoid* acrolein: 1.215 Å), and the hydride−Ru−O and hydride−Ru−C(1) angles are 116.4° and 154.6°, respectively.

Thermodynamics of formation of **4** from the isolated reagents is slightly exothermic by 2.1 kcal/mol. However, $\mathbf{TS_{3-4}}$ lies 55.6 kcal/mol above the reactants, making the process quite unfeasible. It is noteworthy that, if a different (*less stable*) five-coordinated isomer **5** (Figure 6) for the final product is formed, with the C(1) atom *trans* to a vacancy and the hydride *trans* to a phosphine ($|\Delta E(\mathbf{4}-\mathbf{5})| = 3.6$ kcal/mol), the related $\mathbf{TS_{3-5}}$ lies *lower* in energy (29.4 kcal/mol). Therefore, if formation of a Ru−C(1) bond occurred, it would probably go along the latter path, with a much lower energy barrier. However, this latter mechanism seems also quite unfavorable to occur in aqueous solutions.

(ii) In the Ru−H insertion through the C(1) atom, after **2** → **3** rearrangement as discussed above, two species appear as relative minima on the potential energy surface: an agostic Ru−C−H complex (**6**), in which the newly formed C−H bond fills the ruthenium coordination vacancy, and a "C_{4v}-like" pyramidal species [$RuH(PH_3)_3$(η^1-O−CH_2−CH═CH_2)] (**7**) with the organic substrate in an η^1 coordination mode (Figure 7).

Examination of the reaction profile reveals that, starting from the six-coordinated complex **3**, **6** is initially the first intermediate, which forms through $\mathbf{TS_{3-6}}$. The energy barrier for this process is 10.7 kcal/mol, and intermediate **6** (which lies 10.5 kcal/mol above **3**) is very close in energy to the transition state, since the potential energy surface around **6** is quite flat. Then, this intermediate can evolve to the final **7**, through a transition state $\mathbf{TS_{6-7}}$ that lies 5.6 kcal/mol above **6**. Thus, the global barrier for formation of **7** is 16.1 kcal/mol. Figure 8 collects the schematic energy profile for formation of **7** from **3**.

(iii) While exploring the potential energy surface searching for the TS for formation of complex **4** (see Figure 5), a new cyclic structure **8** appeared, with a direct Ru−C(3) bond, where the alcoholic group fills the ruthenium coordination vacancy (Figure 9). The energy of this structure is lower than that of the reactants by 5.3 kcal/mol (compared with **2**). The high stability of this isomer drove us to study an alternative pathway for the hydrogenation process.

A more accurate theoretical analysis showed that **8** forms from **2** in three steps: the first one is a Michael addition of one

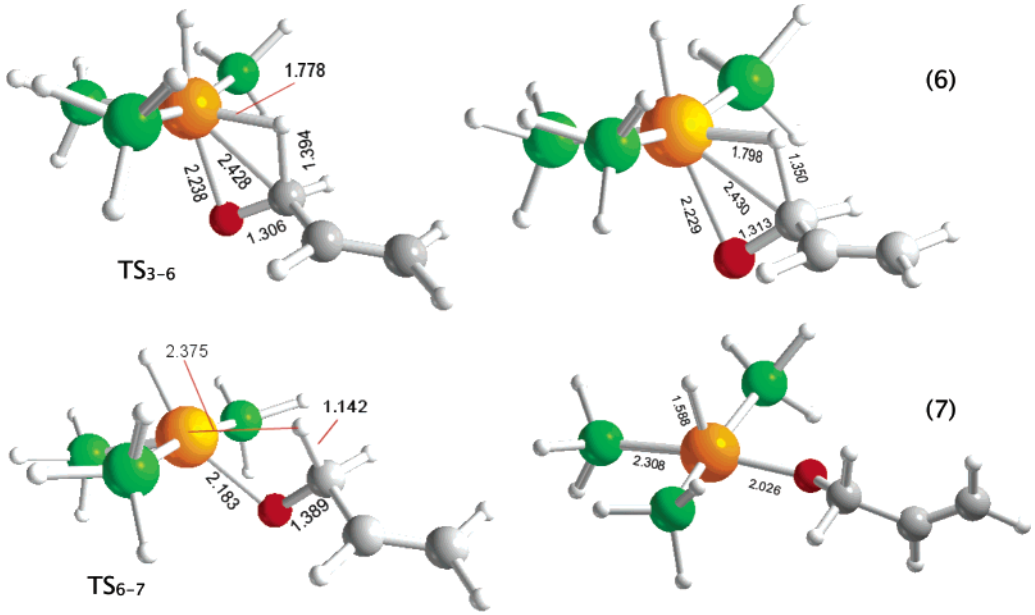

Figure 7. Complexes **6** and **7** and related transition state structures $\mathbf{TS_{3-6}}$ and $\mathbf{TS_{6-7}}$ [selected optimized bond lengths (Å) are reported].

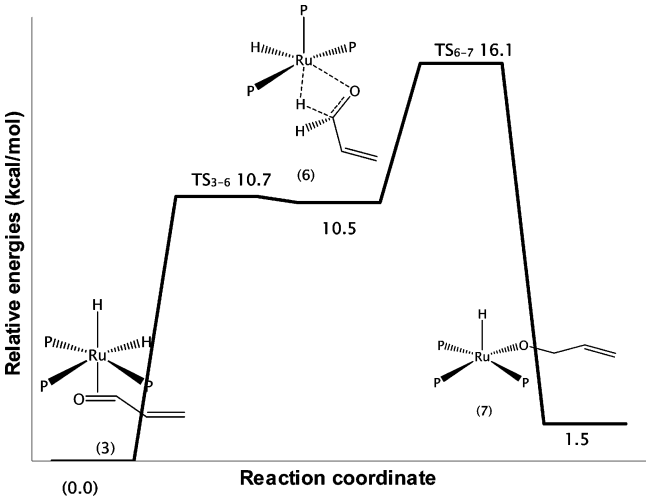

Figure 8. Reaction energy profile for the formation of the square pyramidal $[RuH(PH_3)_3(O{-}CH_2{-}CH{=}CH_2)]$.

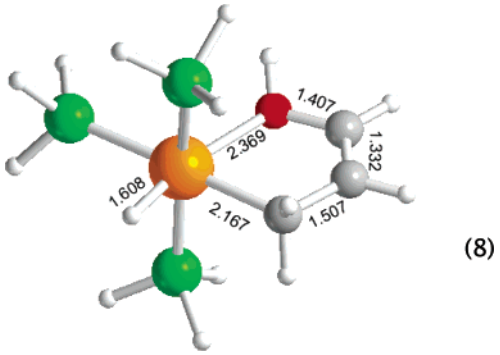

Figure 9. Complex **8** [selected optimized bond lengths (Å) are reported]. The angle O−Ru−C(3) of the five-membered ring is 78.6°.

hydride to the C(3) of the coordinated aldehyde, with formation of the agostic complex **9** (Scheme 2). The energy of the transition state $\mathbf{TS_{2-9}}$ is 16.1 kcal/mol, and the intermediate **9** lies 14 kcal/mol above the starting material.

Structure **9** rapidly evolves to **10** through transition state $\mathbf{TS_{9-10}}$, lying only 1.5 kcal/mol above **9**. Structure **10** is very stable, if compared with **2** ($|\Delta E(\mathbf{2}{-}\mathbf{10})| = 16.5$ kcal/mol). The following step is a (concerted) hydride → O(alcoholate) transfer and a C(3)−H oxidative addition on ruthenium, to form **8** after overcoming a barrier of 43.7 kcal/mol. The highest energy barrier step is the latter, as depicted in Figure 10.

The high value of the energy barrier for the last step is possibly related to the fact that oxidative addition is not typical of the ruthenium metal, especially in aqueous solutions.[12a,b] Intriguingly, **8** is more stable in water than both **5** and **7**, lying 10.6 kcal/mol below the isolated **1** and aldehyde reactants (while **5** and **7** lie 1.5 above and 9.0 kcal/mol below the isolated reactants, respectively). Nevertheless, from the analysis of all the energy barriers obtained, **7** is shown to form more easily, with an energy barrier of 16.1 kcal/mol, referring to the highest TS found in the profile ($\mathbf{TS_{6-7}}$, Figure 8). The highest energy barriers found for the formation of **5** and **8** are 29.4 ($\mathbf{TS_{3-5}}$, Figure 6) and 43.7 (the passage **10** → $\mathbf{TS_{10-8}}$ in Figure 10) kcal/mol, respectively.

1.2. Second Hydrogenation Step: Hydrogen Comes from Water. To close the catalytic cycle, a second hydrogenation step was considered with three different alternatives (always assuming that the starting point is **7**): (i) hydrogen atom coming from complex **7** itself; (ii) hydrogen atom coming from a coordinated H_2 molecule; (iii) hydrogen atom coming *from the solvent* H_2O. The first two mechanisms see the presence of the solvent only as a continuum (CPCM), while in the last case a *discrete* representation *joint to* the continuum model was employed, to mimic the possible direct reaction of water molecules with **7**.

(i) Since the resulting intermediate **7** still possesses a hydride ligand *cis* to the oxygen atom of the organic substituent, it is possible to think about another insertion, similar to that seen before (Scheme 3).

The final product **11** would be a Ru(0) "D_{4h}-like" four-coordinate complex, with the alcohol coordinated through its O atom. Its energy is quite high compared with the starting material ($|\Delta E(\mathbf{7}{-}\mathbf{11})| = 14.8$ kcal/mol); the $\mathbf{TS_{7-11}}$ for this reaction lies 29.6 kcal/mol above **7**. In addition, a change in the metal oxidation state is not observed experimentally throughout the reaction;[12b] therefore we can conclude that this alternative is not realistic.

Scheme 2. Compounds 9 and 10 Forming from 2 [selected optimized bond lengths (Å) are reported][a]

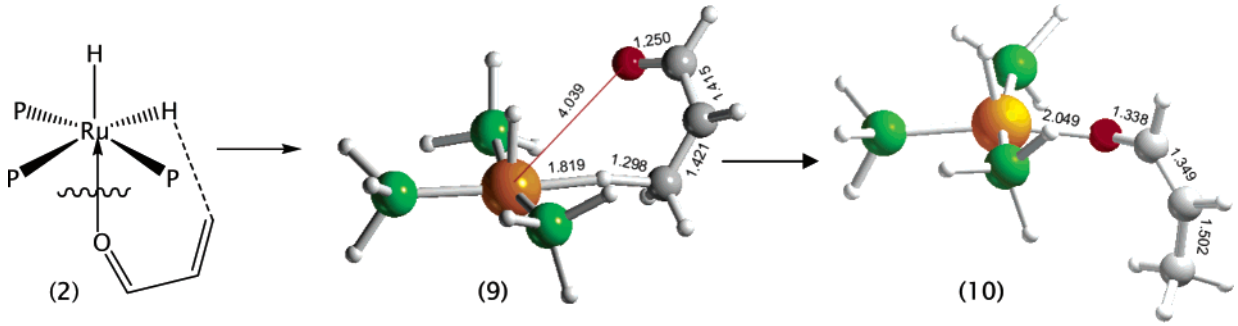

[a] The rotamer appearing in **2** is such that the C(3)−H distance is minimized (3.081 Å).

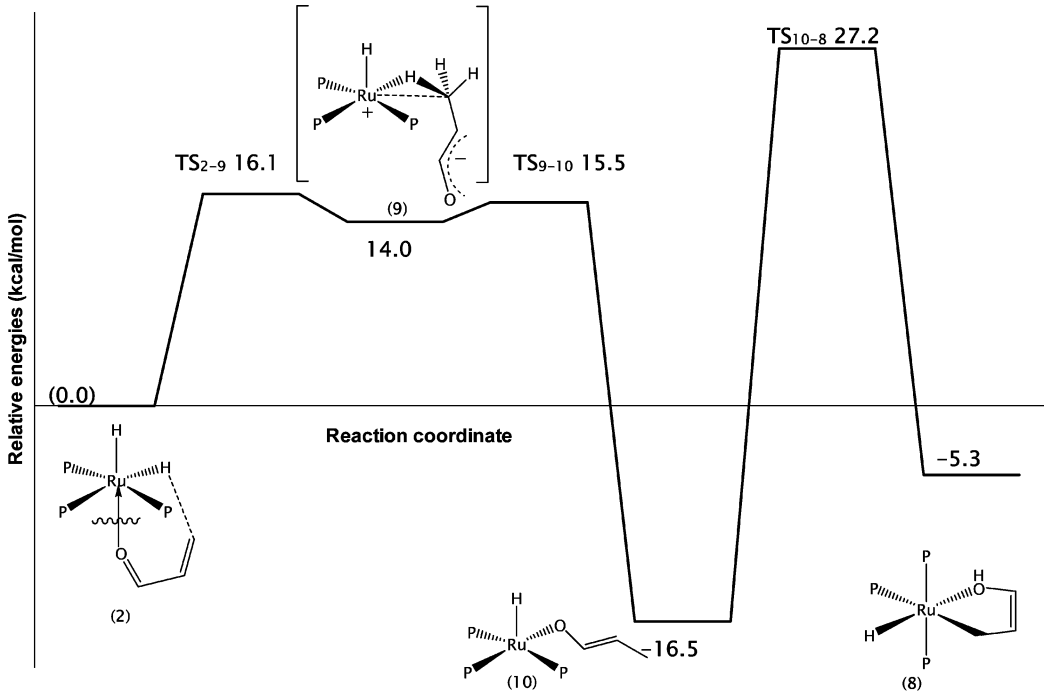

Figure 10. Reaction energy profile for the formation of **8** from **2**.

Scheme 3. Formation of Complex 11 from Precursor 7 [selected optimized bond lengths (Å) are reported][a]

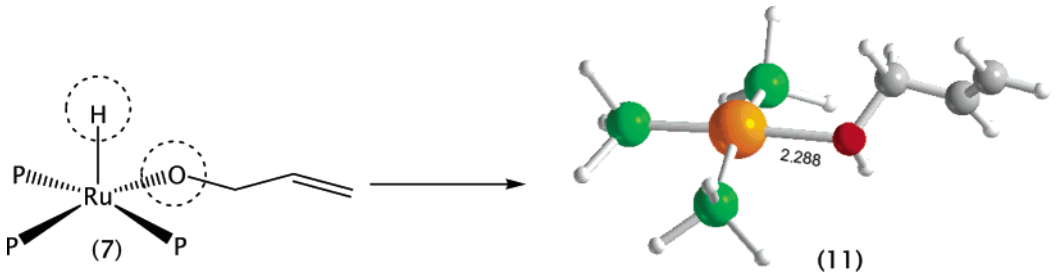

[a] Angles around the ruthenium atom are all around 90°.

(ii) The vacant coordination site on the initial complex can be occupied by an H_2 molecule, to form the dihydrogen complex **12** (Scheme 4). The H−H bond length (0.784 Å) is slightly larger than that in free H_2 (0.743 Å), as a consequence of the d(Ru) → $\sigma^*(H_2)$ back-donation.

The coordination is exothermic by 6.0 kcal/mol, and one hydrogen atom from the coordinated H_2 can migrate to the oxygen atom of the organic ligand (Scheme 5).

This reaction is exothermic by 3.2 kcal/mol; the final product **13** has the alcohol coordinated to ruthenium(II) through an oxygen lone pair. The barrier for this transfer is 13.9 kcal/mol, and the same ruthenium oxidation state is kept through the process. In Figure 11 the transition state $\mathbf{TS_{12-13}}$ is shown.

Alcohol de-coordination from **13** (after overcoming a second barrier of 11.9 kcal/mol, $\mathbf{TS_{13-1}}$) automatically regenerates the active species **1**, closing the cycle. The six-coordinated complex **13** and the isolated products **1** and allylic alcohol are isoenergetic. This can be due to two simultaneous effects, which cancel each other out: de-coordination (an endothermic process) accompanied by rearrangement of the hydride ligands from *trans* to *cis* (exothermic, since the *cis* isomer is more stable). Thus, the highest barrier for the conversion **7** → **1** would be 13.9 kcal/mol. The overall energetic profile is shown in Figure 12.

(iii) Another plausible option is to think about a direct reaction of **7** with water molecules, whose concentration is much higher than that of H_2. **7** has a vacant site in a position *trans* to the

Scheme 4. Formation of the "Nonclassical" Ruthenium−Dihydrogen Complex 12 [selected optimized bond lengths (Å) are reported]

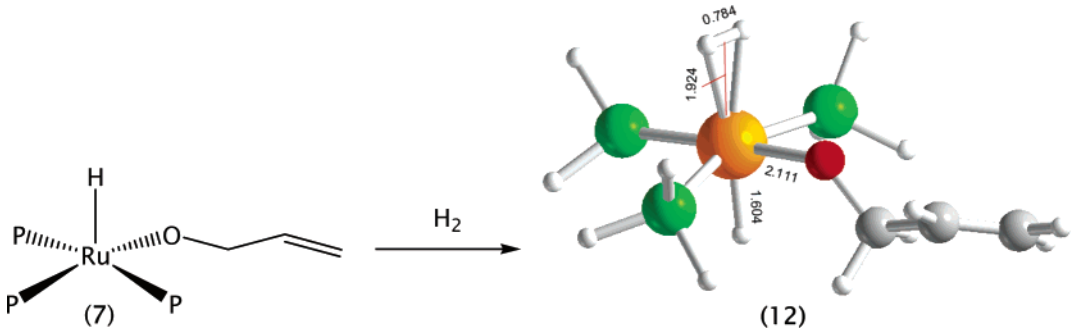

Scheme 5. Formation of Complex 13 from "Nonclassical" Ru-Dihydrogen Complex 12 [selected optimized bond lengths (Å) are reported]

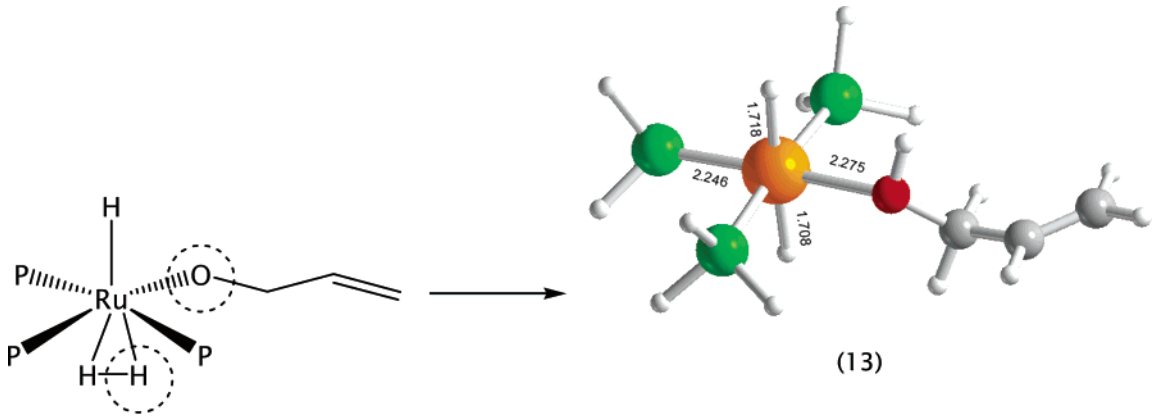

hydride, which can be occupied by a water molecule, to form the aqua complex **14** (Figure 13).

The stabilizing coordination energy is 8.5 kcal/mol, and the water molecule interacts with the O-bound organic substituent, via a hydrogen bond. To describe the solution environment, the cluster $(H_2O)_3$ was used to mimic the behavior of the solvent molecules around the active site (see Computational Details). The related system **15** was the starting point for the calculations concerning the O-protonation of the coordinated substrate with water (Figure 14).

The hydrogen atom that is transferred is not coming from the bound water molecule, since its hydrogens are too far away from the oxygen of the alcoholate ligand [mean distance ca. 3.0 Å; now they are much further than in the isolated complex **14** (1.647 Å) because of the new interactions with the cluster water molecules]. It is more appropriate to think about a transfer from one water molecule coming from the bulk (the cluster itself in our case), the hydrogens of which are much closer in space to the O-bound substituent (Figure 14). In addition, it is more reasonable that, given the large number of water molecules around the complex, the solvent itself is directly interacting with **7** rather than the aqua ligand.

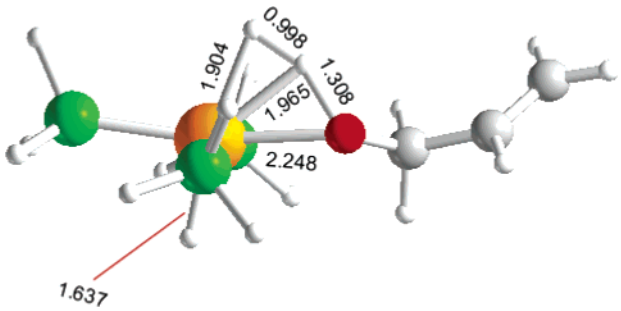

Figure 11. TS_{12-13} [selected optimized bond lengths (Å) are reported].

Thermodynamics for the proton transfer is endothermic by 6.3 kcal/mol. Calculation of the energy barrier for the process in this case cannot be exact, since charge separation occurs, with the formation of hydroxide ions after protonation. To estimate the transfer energy, restricted optimizations were made, fixing the O(alcoholate)- - -HOH distance at different values between 1.6 Å (found in complex **15**) and 1.0 Å (final hydrogenated species **16**). The related CPCM profile is shown in Figure 15.

It was found that the application of the continuum does not exhibit a large effect on the total energy change for this process. This suggests that *only the first solvation sphere* plays a significant role in the process. Figure 15 shows that there are no inflection points on this curve; therefore the energy barrier was only *approximately estimated* through the thermodynamic energy difference. The computed energy shows that the protonation of the formed alkoxide intermediate by a bulk water molecule entails a low energy cost. The final ruthenium(II) complex **16** (where the cluster $[(OH)(H_2O)_2]^-$ has been removed) bears a positive charge (Scheme 6).

At this stage, for the reaction to proceed, one of the ligands should decoordinate to generate a coordination vacancy on the metal center. Two different options are conceivable: either the water or the alcohol molecule can dissociate, to let an H_2 molecule coordinate to the metal and close the catalytic cycle.

For this ligand dissociation process thermodynamics favors water dissociation: ΔE(**16**→**18**+H_2O) = +17.5kcal/mol, while ΔE(**16**→**17′**+alcohol) = +20.7 kcal/mol. Dissociation of a water molecule (a ligand *trans* to hydride) is energetically more favorable than the alcohol dissociation (a ligand *trans* to a

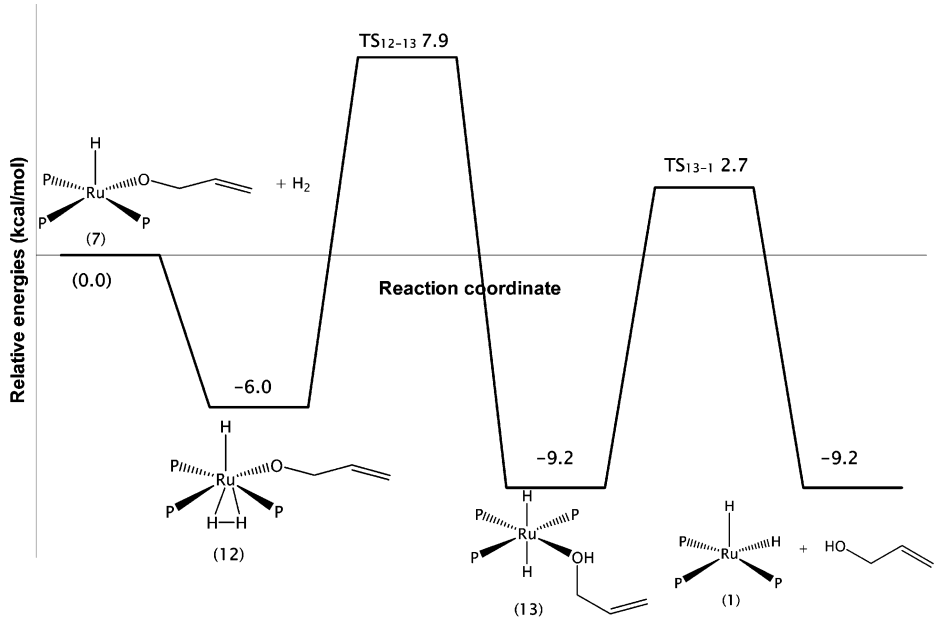

Figure 12. Reaction pathway for the direct hydrogenation by H_2.

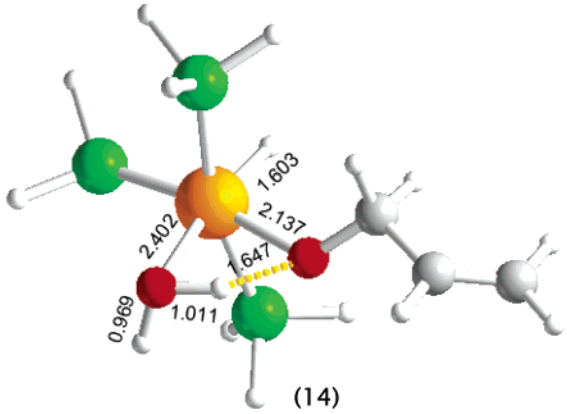

Figure 13. Aqua complex [RuH(H_2O)(PH_3)$_3$(O−CH_2−CH═CH_2)] (**14**) [selected optimized bond lengths (Å) are reported].

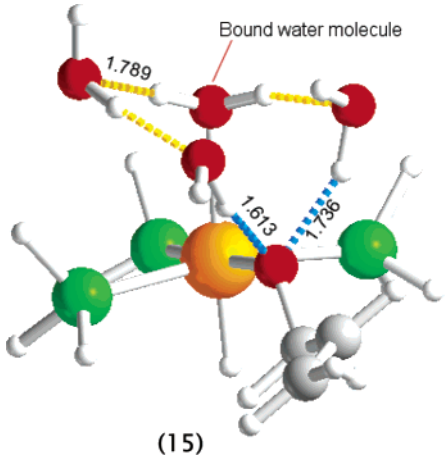

Figure 14. Complex **14**·(H_2O)$_3$ (**15**). The bound water molecule now forms new H-bonds with the water cluster. In light blue the closest HOH- - -alcoholate contacts are highlighted (Å).

phosphine). Nevertheless, examination of the energy profile for Ru−alcohol bond lengthening shows that in this case an additional *rearrangement* of the five-coordinated species may occur, to get a final geometry with a vacancy *trans* to the hydride ligand, stabilizing the system by 6.6 kcal/mol (complex **17**, Scheme 6). This rearrangement is not needed in the case of **18**, where the ligand decoordinated is already *trans* to the hydride. Therefore we can assume that the energy barrier to obtain complex **17′** is higher than that needed to obtain **18**. The relative *trans* influences of the hydride and phosphine ligands in **16** cause the Ru−water bond to be longer than the Ru−alcohol bond (2.400 vs 2.246 Å).

H_2 coordination will take place on **18**, and the process is exothermic by 9.0 kcal/mol. To close the catalytic cycle, further H_2 deprotonation is needed, and it can only be accomplished by the solvent. The cluster $[(OH)(H_2O)_2]^-$ was introduced to represent the basic medium, where the solvated hydroxide anion acts as the base. $[(OH)(H_2O)_2]^-$ was applied on the basis of similar considerations that led to the application of the $(H_2O)_3$ cluster; that is, single OH^- would have been an unrealistic representation of basic aqueous solutions (see Computational Details). The model system **19** and the related reaction is drawn in Scheme 7.

It was not possible to obtain structure **19** as a minimum, because when the complex and the cluster are put next to each other, a spontaneous neutralization between the two oppositely charged bodies occurs, by moving a proton from the coordinated H_2 to the OH^- group, forming **20**. Once again, as already seen for complex **15**, the transition state for this step cannot be evaluated exactly, due to "charge neutralization". Therefore, an energy profile similar to that of Figure 15 was calculated in this case too, varying the H−H distance in the coordinated H_2 and optimizing with the frozen bond constraint. It was assumed that *d*(H−H) in **19** is the same as that found in the *isolated* (nonsolvated) [RuH(η^2-H_2)(PH_3)$_3$(alcohol)]$^+$ (0.79 Å). The potential energy curve is shown in Figure 16.

Thermodynamics for this process is very favorable: in water the conversion is exothermic by 18.2 kcal/mol [to work out the ΔE value for the reaction, the energy of **19** was approximated by the sum *E*(*isolated* cationic ruthenium complex) + *E*(*isolated* anionic cluster)]. No activation barrier could be found, at least judging from the profile.

Another option is to consider water as a base instead of OH^-, and this hypothesis was tested as well, using the cluster seen before, $(H_2O)_3$ (Scheme 8). In this case, despite the fact that there are no charge separation/neutralization problems, it was

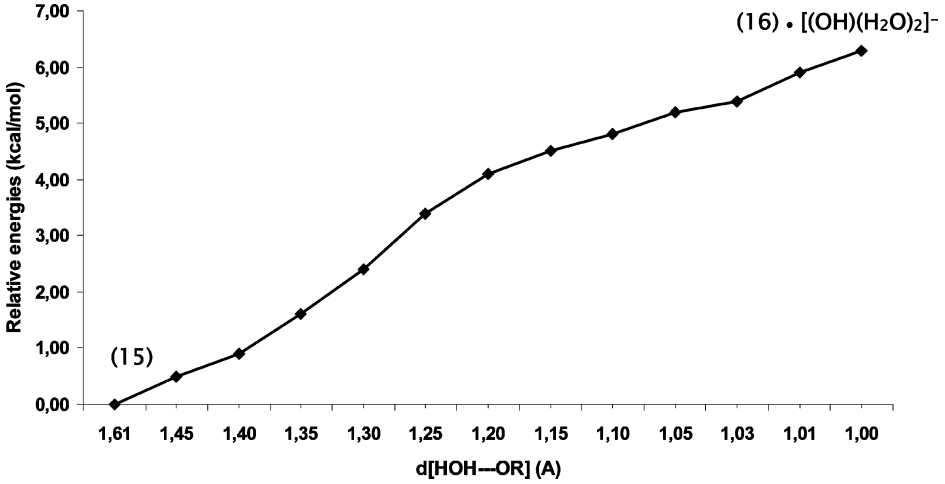

Figure 15. Energy profile for variation of the HOH- - -OR distance in **15**.

Scheme 6. Two Possible Alternatives for Ligand Dissociation from 16

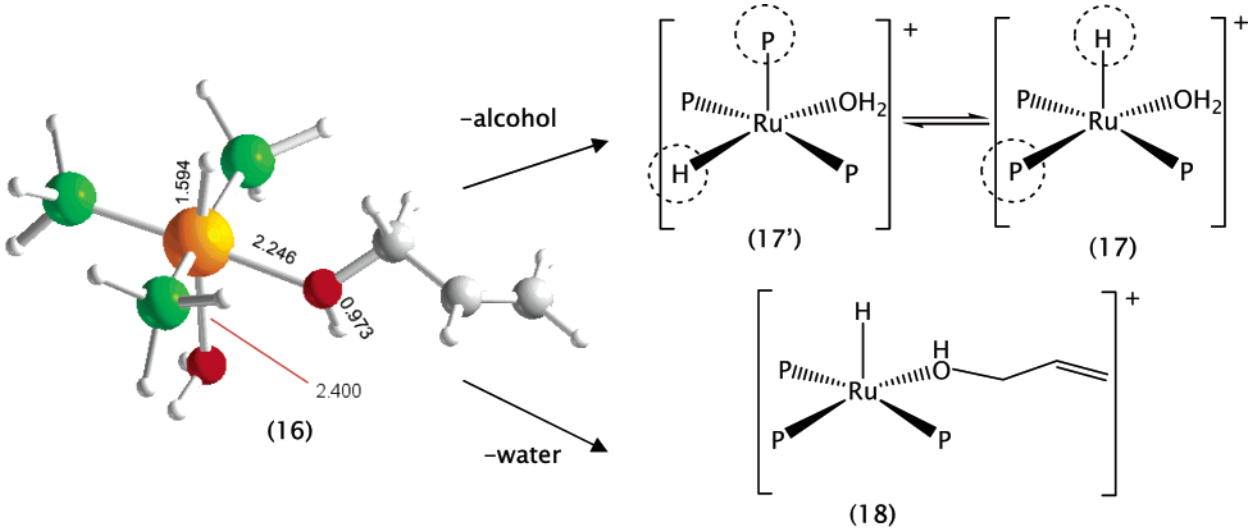

Scheme 7. Deprotonation of Coordinated H_2 in 19 by the Cluster $[(OH)(H_2O)_2]^-$ to Give Structure 20 [selected optimized bond lengths (Å) are reported][a]

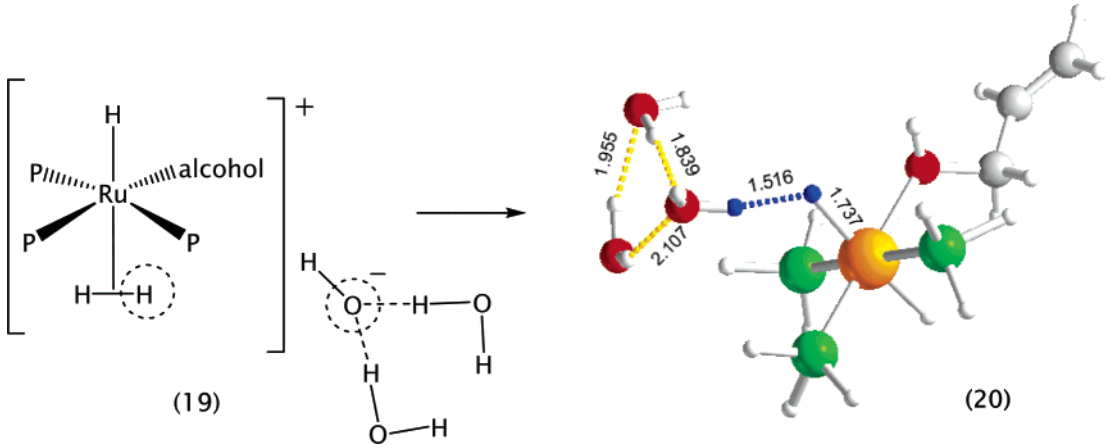

[a] The hydrogen atoms coming from the original H_2 ligand are drawn in blue.

not possible to locate *the product* as a minimum on the potential energy surface; all the optimization attempts led to the starting material. Thermodynamics in this case tells that the reaction is *endothermic* by 24.7 kcal/mol in water [again, taking *E*(*isolated* neutral ruthenium complex) + *E*(*isolated* cationic cluster) as an approximation of the product energy, right-hand side of Scheme 8]. Thus, whereas the reaction with water as a base is endothermic and the reaction spontaneously goes to the left (Scheme 8), for the reaction using OH^- the reaction proceeds with no barrier to form the product (Scheme 7). Given the point that the reaction takes place in basic conditions, the energy barrier for this deprotonation should not be important according to the spontaneity of the calculated reaction.

The final part of the cycle is analogous to that of subsection

Scheme 8 Alternative (but unfavorable) Deprotonation of $[RuH(\eta^2\text{-}H_2)(PH_3)_3(alcohol)]^+$ Using $(H_2O)_3$

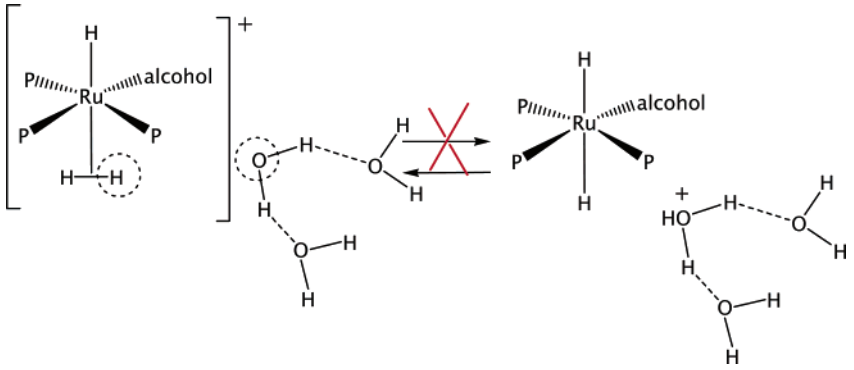

(ii): alcohol decoordination from **20** (which is equivalent to **13** when the solvent ligand is removed) after overcoming a barrier corresponding to $\mathbf{TS_{13-1}}$ permits closing the catalytic cycle and forming the active species *cis*-$[RuH_2(PH_3)_3]$ again.

2. Catalysis with *cis*-$[RuH_2(PH_3)_4]$ ("P_4" mechanism). 2.1. First Hydrogenation Step. Experimental evidence showed that the major species in basic solution is the octahedral complex *cis*-$[RuH_2(m\text{tppms})_4]$; thus an alternative way to catalyze the hydrogenation was taken into account, starting from the coordinatively saturated species. $[RuH_2(PH_3)_4]$ was the model, and catalyst isomerism was examined first, since octahedral $[RuH_2(PH_3)_4]$ may exist in a *cis* and a *trans* dihydride form (Figure 17).

Calculations showed that the *cis* isomer **21** is more stable than the *trans* by 9.7 kcal/mol, as it is also confirmed by XRD data: all the crystallographically characterized $[RuH_2P_4]$-type complexes ($[RuH_2(PMe_3)_4]$[29] or $[RuH_2(PPh_3)_4]$[30] for example) show a *cis* disposition of the two hydride ligands. Thus, this isomer was taken into account in the following steps. Figure 18 shows the optimized structure of *cis*-$[RuH_2(PPh_3)_4]$ (**21-PPh$_3$**). A comparison of selected calculated structural parameters for **21** and **21-PPh$_3$** is given in the Supporting Information.

Interaction of acrolein with *cis*-$[RuH_2(PH_3)_4]$ leads to two possible reaction intermediates, once a hydrogen is transferred to either the C or the O atom of the C═O group (and assuming that the hydrogen atoms required for reduction are coming from the complex itself and not from free H_2 or from water). Both structures of the O-bound (**22**) and C-bound (**23**) carbonyl have been optimized, and the first one is more stable, lying 1.3 kcal/mol above the reactants (Figure 19). The second one lies 6.7 kcal/mol above the reactants. Thus both reactions are endothermic.

The transition states for this step ($\mathbf{TS_{21-22}}$ and $\mathbf{TS_{21-23}}$, Figure 20) lie 26.8 and 56.3 kcal/mol above the reactants, respectively. From these very high values it can be inferred that both reactions seem unfeasible; nevertheless, the one leading to the (most stable) O-bound intermediate is much more favorable. In $\mathbf{TS_{21-23}}$ the hydrogen atom is almost at the same distance from either the C or the O atom of the carbonyl group, suggesting that there is a sort of "H-jump" to the C═O double bond rather than to the specific oxygen atom. Subsequent IRC analysis though confirmed the final O−H [and simultaneous Ru−C(1)] bond formation from $\mathbf{TS_{21-23}}$.

From the comparison of these barriers with those obtained in section 1, it is clear that the "P_3" mechanism is much more feasible, because the transition states found for the first catalytic step lie much lower in energy than those found for the "P_4" mechanism: cf. 26.8 versus 5.4 kcal/mol for the O-bound (species **22** and **7**) or 56.3 versus 29.4 kcal/mol for the C(1)-bound (species **23** and **5**) intermediates, respectively. As a consequence, catalysis with *cis*-$[RuH_2(PH_3)_4]$ was not analyzed further.

3. The Proposed Mechanism. On the basis of the extensive investigation of the possible reaction routes of C═O hydrogenation catalyzed by water-soluble phosphine complexes of ruthenium, we found that the most plausible reaction mechanism is

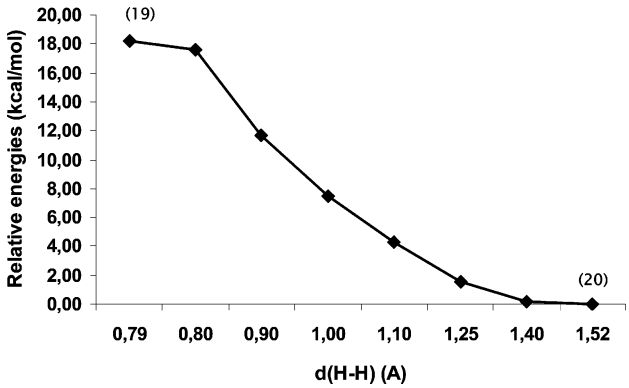

Figure 16. Energy profile for the reaction **19** → **20**.

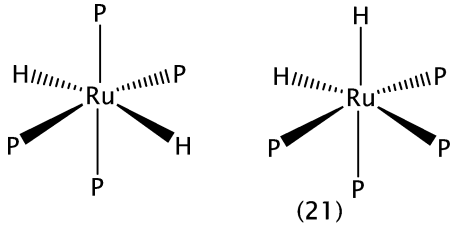

Figure 17. Different isomers of $[RuH_2(PH_3)_4]$.

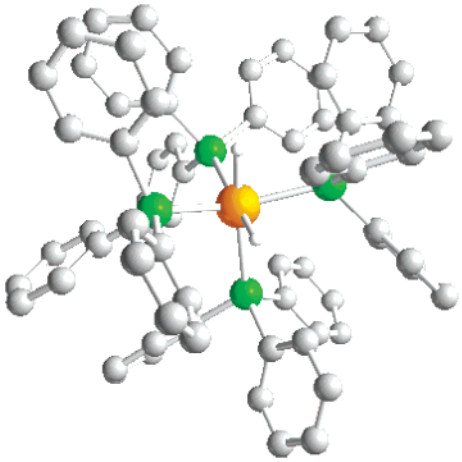

Figure 18. Optimized structure of **21-PPh$_3$** (hydrogen atoms on the phenyl rings were omitted for clarity).

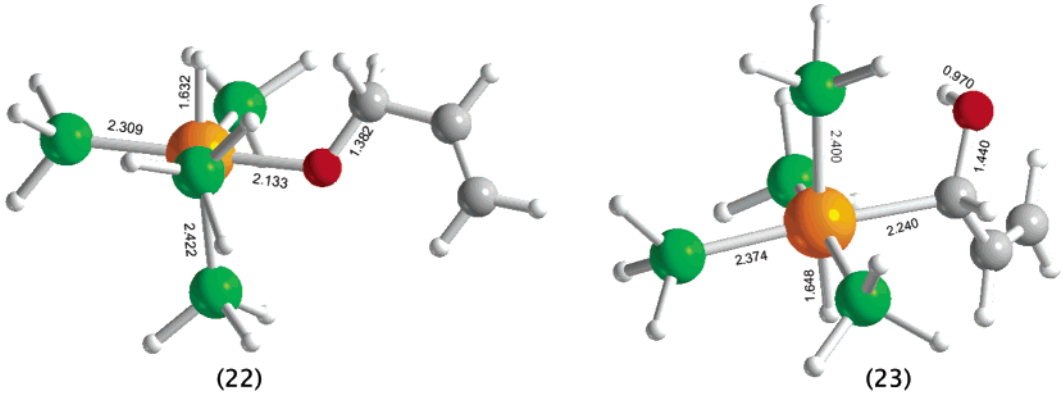

Figure 19. Complexes **22** and **23** [selected optimized bond lengths (Å) are reported].

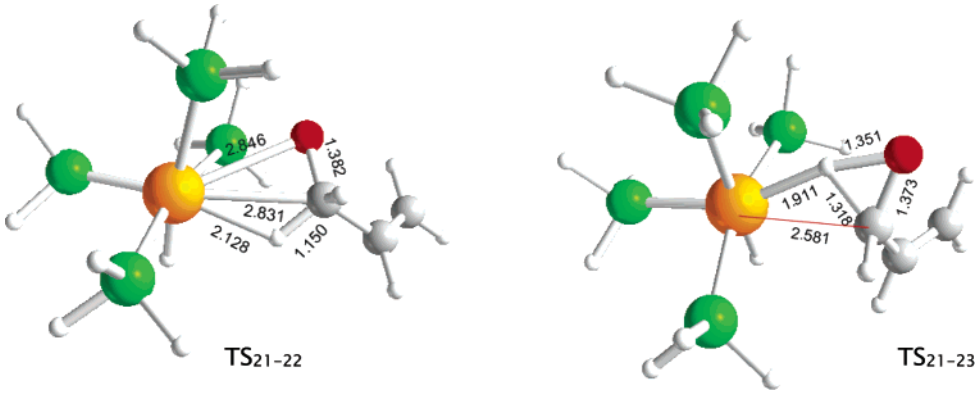

Figure 20. TS_{21-22} and TS_{21-23} [selected optimized bond lengths (Å) are reported].

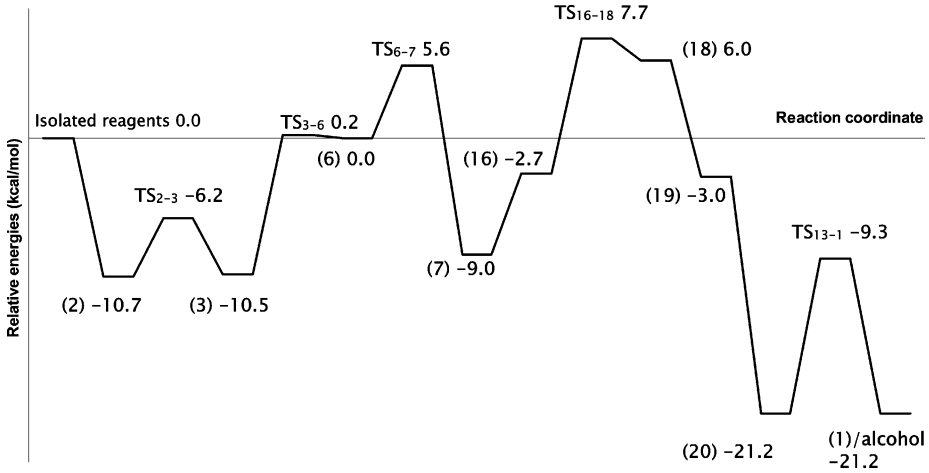

Figure 21. Global energy profile for the conversion of acrolein to allyl alcohol.

as follows (Scheme 9). In agreement with other theoretical works[18,19,27b] the "RuH_2P_3" type complex, formed by the dissociation of a phosphine ligand from the spectroscopically detected "RuH_2P_4" complex has to be the first reaction step, since the reaction barriers for the reduction were found to be much lower in the case of the "RuH_2P_3" intermediate. The next step is the coordination of the aldehyde through its C═O bond, which is followed by the insertion of the C═O group into the Ru−H bond. On the basis of the calculations and other considerations the second hydrogen should come from the solution, and the calculations show that this can easily happen by the transfer of a proton from the surrounding water molecules (see Figure 15). The catalytically active intermediate can be regenerated by the coordination and subsequent deprotonation of an H_2 molecule followed by the dissociation of the product from the complex.

Figure 21 reports the overall energy profile of the conversion of acrolein to allyl alcohol in the context of the "P_3" mechanism.

The mechanism proposed by Delbecq and co-workers[19] also provides a possible reaction route for the C═O hydrogenation, in which they suppose a concerted addition of a hydride ligand and a proton from a coordinated aqua ligand to the C═O bound (water-assisted mechanism). However, even though their proposal is in principle reasonable, we are not fully convinced about that mechanism because in our opinion it does not easily account for the pH-dependent regioselectivity observed in the reaction. Hence, the free energy barriers found for C═O and C═C reductions in basic conditions were similar, 55 and 52 kJ/mol,

(29) Dahlenburg, L.; Frosin, M. *Polyhedron* **1993**, *12*, 427.
(30) Immirzi, A.; Luccarelli, A. *Cryst. Struct. Commun.* **1972**, *1*, 317.

Scheme 9. Proposed Catalytic Cycle for C═O Selective Hydrogenation by *cis*-[$RuH_2(PH_3)_3$]

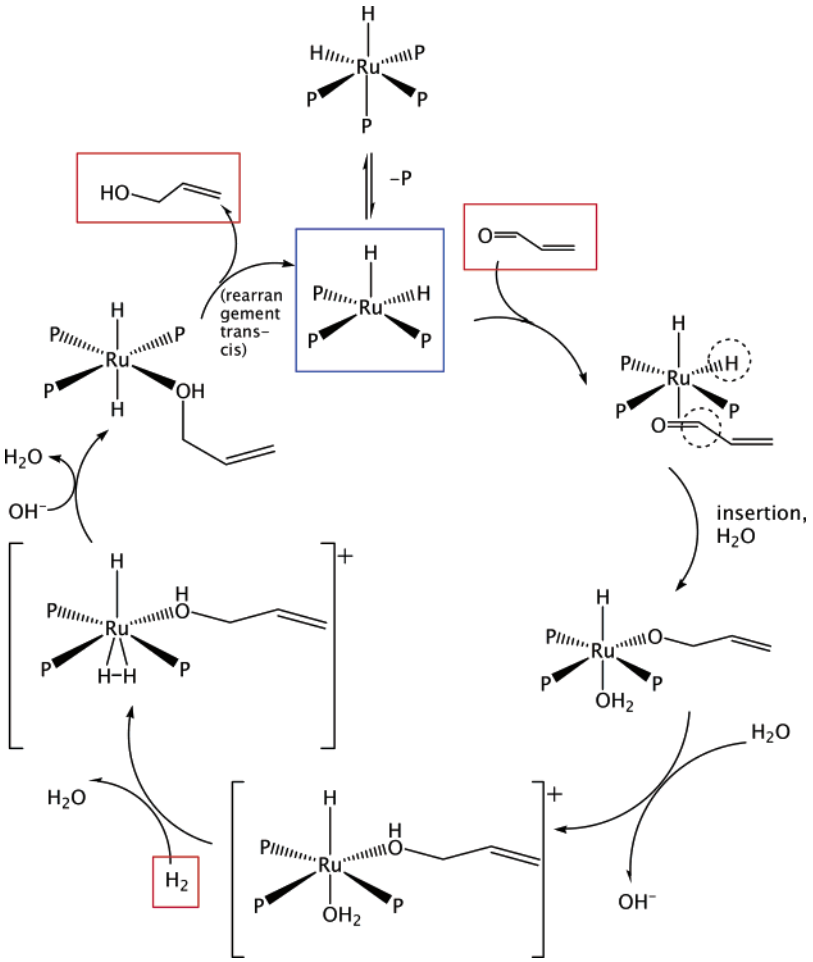

respectively.[19] In addition, in acidic conditions, where the active catalytic species is the [RuHCl(*m*tppms)$_3$] complex, one can envisage an aquo complex [RuHCl(H_2O)(*m*tppms)$_3$] with the H_2O and H ligands in *cis* position also capable of reducing the aldehyde in a similar way to that in basic conditions; nevertheless, in acidic conditions the observed product is the C═C reduction instead of the C═O reduction product. Furthermore, as shown by us earlier,[27a] in acidic solution considering a single water molecule in a proton transfer reaction (as it is shown in the proposed mechanism[18]) cannot provide reasonable energetics.

The mechanism proposed here, however, does account for the regioselectivity in acidic conditions, and a similar reactivity pattern (with the solvent directly involved in the reaction mechanism) was found in a previous study[18] for the regioselectivity in basic conditions.

4. Selectivity of the Hydrogenation in Basic Solutions: Why the Olefinic Bond Is Not Reduced. After the examination of the mechanism of the carbonyl hydrogenation, additional "cross-test" studies were performed, trying to rationalize the observed regioselectivity. Olefin coordination to the metal center was considered to be necessary to start the catalytic reaction, since for C═O hydrogenation the barriers related to the "P_4" mechanism (section 2) were higher than those observed for the "P_3" case (section 1). Thus, precursor **1** was chosen as the starting complex for this analysis.

Coordination of acrolein through its C═C bond to **1** gives complex **24**, with a strong stabilization energy (−26.1 kcal/mol). Lengthening of the C═C double bond is observed after coordination [cf. *d*(C═C) = 1.405 Å in **24** with *d*(C═C) = 1.338 Å in the free aldehyde], because of metal back-donation. Subsequent hydrogen transfer to the C(3) occurs with a barrier of 10.3 kcal/mol, to give the agostic intermediate **25**, which lies at 7.6 kcal/mol above **24** (Scheme 10). Transfer of hydrogen to the C(2) was examined in the theoretical study of the selective C═C reduction catalyzed by [{$RuCl_2$(*m*tppms)$_2$}$_2$] in acidic solutions,[18] and it was proved to be less favorable, both for the model acrolein and the real cinnamaldehyde; therefore only the C(3) transfer was considered in here.

The first hydrogenation step is still feasible, and there is practically no difference between the barrier found in this case and that found for the C═O case [10.7 kcal/mol for agostic **6** formation, section 1.1, case (ii)]. Therefore, the kinetics of this step does not account for the selectivity.

The second hydrogenation cannot involve the other hydride ligand of **25**, since it is *trans* to the C(2) atom of the aldehyde. Another possibility would be the coordination of a H_2 and then a metathesis reaction between the carbon−carbon bond and the coordinated H_2. It was shown that this reaction does not have a high energy barrier either in the case of the C═C reduction[18] or in the case of C═O reduction;[19] however the reaction occurring this way would not account for any selectivity as a function of pH; in addition, the concentration of H_2 is much lower in the solution than that of solvent molecules. Thus, the reaction is unlikely to proceed this way, and hence interaction of **25** with the solvent environment has to be considered. As already seen for the case of system **15**, the cluster $(H_2O)_3$ was introduced (a new system **26** was built), and the barrier is estimated only with the same criteria as those already described

Scheme 10. Formation of the Agostic Complex 25 from [$RuH_2(PH_3)_3(\eta^2$-κ,C-κ,C-acrolein) (24) [selected optimized bond lengths (Å) are reported][a]

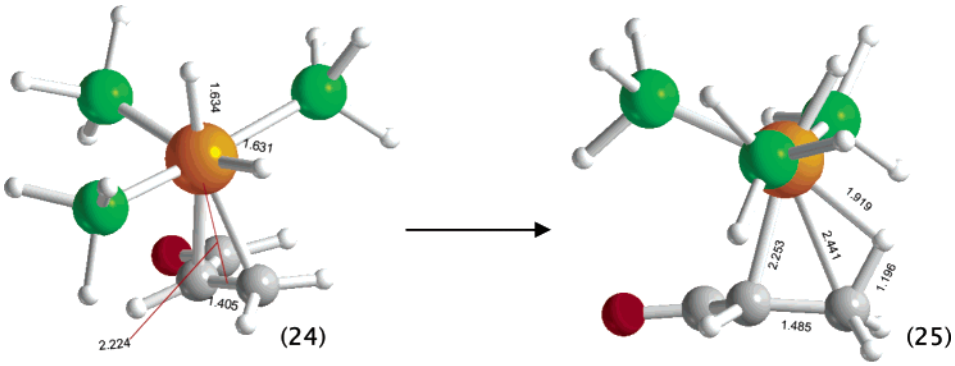

[a] In 24 the H−Ru−H angle is 75.0°.

Scheme 11. Transfer of a Proton (drawn in blue) from a Water Molecule to the Coordinated C(2) in Complex 26 = 25·$(H_2O)_3$ [Selected optimized bond lengths (Å) are reported][a]

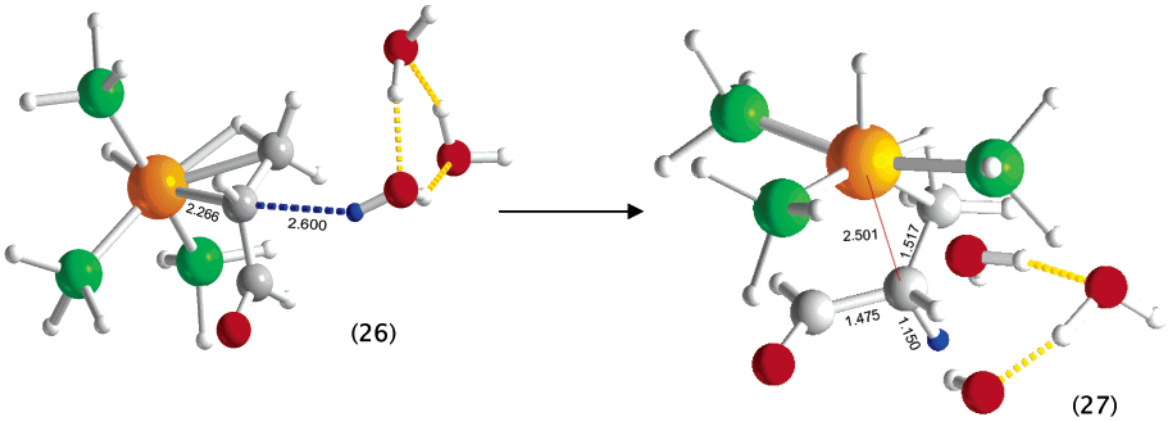

[a] After the process, the protonated C(2) leaves the ruthenium coordination sphere.

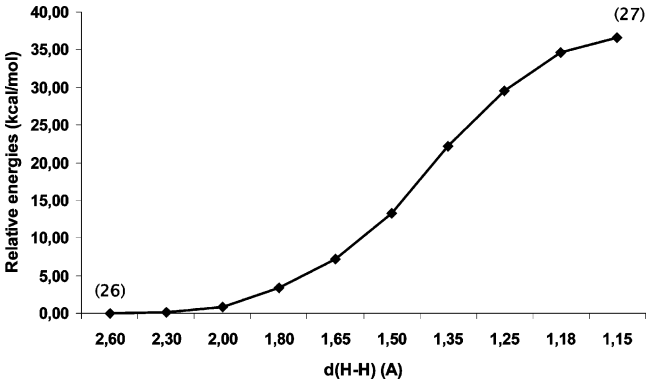

Figure 22. Energy profile for the reaction **26** → **27**.

before, since charge separation occurs. The conversion considered is shown in Scheme 11.

An evaluation of the energy barrier was done along the same criteria as before; the graph reporting the (relative) energy versus the frozen C(2)−H distance is reported (Figure 22). Values are between 2.60 Å (optimized value in the reactant) and 1.15 Å (optimized value in the product).

In this case the energy rises smoothly, and no transition state could be found. Nevertheless, the thermodynamics of the conversion shows that the reaction is strongly endothermic by 36.6 kcal/mol, possibly justifying the lack of C═C hydrogenation under basic conditions. The transfer of a proton from a water molecule to the C═C bond requires *at least* 36.6 kcal/mol, which is much more than the highest barrier found for C═O hydrogenation (16.1 kcal/mol). Therefore this can confirm why selective hydrogenation of C═O bonds of cinnamaldehyde was observed with [{$RuCl_2$(*m*tppms)$_2$}$_2$] in basic solutions. In acidic solutions protonation of the second carbon is a much more favorable process, since under acidic conditions the effective protonating agent is H_3O^+, a much stronger "proton donor" than H_2O, the protonating agent in basic conditions. The calculations for acidic pH conditions[18] showed that protonation of the second carbon atom with $[H_3O(H_2O)_2]^+$ has an activation barrier of less than 10 kcal/mol, accounting for fast C═C hydrogenation in acidic aqueous solutions.

Conclusions

The theoretical investigations described above led to a significant insight into the reaction mechanism of the selective C═O reduction of cinnamaldehyde catalyzed by [{$RuCl_2$(*m*tppms)$_2$}$_2$] (in the presence of excess *m*tppms) in basic aqueous solutions. Our work not only provided a possible mechanism for the C═O reduction but led to convincing rationalization of the selectivity against C═C reduction under these conditions.

The reaction mechanism was constructed by applying PH_3 ligands instead of the sulfonated aromatic phosphines and acrolein as a model for cinnamaldehyde. In the cases where the truncation of the real system seemed to cause significant errors in the energetics (e.g., phosphine dissociation), calculations with aromatic phosphine ligands (PPh_3) were made. The solvent effects of water molecules were also considered. In the cases when solvent molecules or ions can participate in the reaction, we applied small water clusters, which had been

systematically tested in earlier works. In addition, the effect of the bulk solvent was estimated by the application of the conductor-like polarizable continuum model (CPCM/UAKS).

In particular, judged from the data obtained, it seems that *the real "catalytically active" species is a trisphosphine complex, cis-[RuH$_2$(mtppms)$_3$]*, since the energetic profiles for *cis*-[RuH$_2$(PH$_3$)$_3$] give lower activation barriers than those for *cis*-[RuH$_2$(PH$_3$)$_4$]. Easy phosphine dissociation can open a new route to C═O hydrogenation, under more favorable conditions. In addition, the reaction proceeds via O-bound rather than C-bound intermediates. The first hydrogen atom that adds to the carbon of the C═O group is the hydride ligand of the catalyst, while on the basis of the calculations the second one is thought to come directly from the solvent. Molecular H_2 is also needed to regenerate the active species and close the catalytic cycle, after the formation of allylic alcohol. Besides being active in the protonation of the alcoholate ligand of **14**, water (in its "basic" OH^- form) also gives a very exothermic deprotonation of the coordinated H_2 in **19**.

Calculations revealed again that water is a rather unconventional reaction medium for organometallic catalysis, since water molecules can play important roles in many reaction steps. Water can coordinate to the metal center and can occupy the vacant sites in the reactants or intermediates. In addition water and its ions can take part in proton transfer reactions along the reaction path and provide alternative mechanistic possibilities, which would not be available for reactions in nonpolar and noncoordinating organic solvents.

The observed selectivity for C═O reduction of this catalyst was explained by performing the "cross-test" reaction of C═C hydrogenation on the same *cis*-[RuH$_2$(PH$_3$)$_3$]. Results show that first hydrogenation reduction of the C═C double bond by the transfer of one of the hydride ligands of the complex is feasible because the TS for this step lies more or less as high in energy as that of the analogous step for C═O reduction. This step leads to a metal/C−H agostic interaction, thus saturating the ruthenium coordination sphere. Consequently, the second hydrogen must come directly from the solvent, since no coordination vacancies that could host other reducing species are available on the ruthenium center. Therefore, a water solvent molecule must be the protonating agent. For the C═C protonation by water, the estimated thermodynamic energy difference between reactant and product is too high for the reaction to occur. These results also indicate that the second hydrogenation step for the polar C═O bond is much easier than for the (nonpolar) C═C bond, in line with the nature of the process: a *proton* transfer. The proton reacts more easily with the more electronegative oxygen atom. The selective C═O reduction in basic media is justified by the fact that the protonating agent is a solvent molecule; water can protonate the polar C═O bond but is not able to transfer a proton to the C═C bond. In acid solution, however, the proton also comes from the media, but the protonating agent is H_3O^+, strong enough to protonate the C═C bond.

To sum up, the above work and the one published earlier by Kovács et al.[18] have provided a complete picture for the selective hydrogenation reactions of α,β-unsatured aldehydes, found in acidic or basic aqueous (aqueous−organic biphasic) reactions. Computational methods including explicit consideration of a cluster of solvent molecules are able to give a microscopic picture of the organometallic reactivity in water. It was found that in acidic solution selectivity arises from the much lower barrier found for the insertion of C═C bonds (than that of C═O bonds) into the Ru−H bond.[18] In contrast, in basic solutions selectivity is much more the effect of the solvent environment, since protonation by water of the O-bound intermediate formed after the insertion of the C═O group into the Ru−H bond has favorable energetics. Conversely, protonation of the C═C bond is not facilitated by water molecules; that is, hydroxonium ions are required, which are present only in acidic solutions in reasonable concentration.

Acknowledgment. This work was supported by the Spanish MEC, grant no. CTQ2005-09000-C02-01, and "Ramon y Cajal" contract to G.U., and Generalitat de Catalunya, project 2005/SGR/00896. Thanks are due to EU program AQUACHEM (http://www.iccom.cnr.it/aquachem/) for financial support (MRTN-CT-2003-503864) and a postdoctoral fellowship to A.R. The Centre de Supercomputació de Catalunya (CESCA) is also thanked for providing additional computational resources. F.J. is grateful for the support of the Hungarian National Research Fund (OTKA T043365 and TS044836). G.K. acknowledges support from the HPC-EUROPA project (RII3-CT-2003-506079), with the support of the European Community−Research Infrastructure Action under the FP6 "Structuring the European Research Area" Programme.

Supporting Information Available: (i) Tables of the optimized geometries (Cartesian coordinates) and total energies for the calculated species. (ii). Selected calculated bond lengths and bond angles for *cis*-[RuH$_2$(PR$_3$)$_3$] and *cis*-[RuH$_2$(PR$_3$)$_4$] (R = H, Ph). This material is available free of charge via the Internet at http://pubs.acs.org.

OM060353S